MOLECULAR IMAGING AND BIOLOGY

Published Online: 10 December 2009

Mol Imaging Biol (2010) 12:500–508
DOI: 10.1007/s11307-009-0290-4

RESEARCH ARTICLE

A Comparison Between Time Domain and Spectral Imaging Systems for Imaging Quantum Dots in Small Living Animals

Adam de la Zerda,[1,2] Sunil Bodapati,[1] Robert Teed,[1] Meike L. Schipper,[1] Shay Keren,[1] Bryan R. Smith,[1] Johnny S. T. Ng,[4] Sanjiv Sam Gambhir[1,3]

[1]*Department of Radiology, Molecular Imaging Program at Stanford (MIPS), The Bio-X Program, Stanford, CA, 94305, USA*
[2]*Department of Electrical Engineering, Stanford University, Stanford, CA, 94305, USA*
[3]*Department of Bioengineering, Stanford University, Stanford, CA, 94305, USA*
[4]*Stanford Linear Accelerator Center, Stanford University, Stanford, CA, 94305, USA*

Abstract

Purpose: We quantified the performance of time-domain imaging (TDI) and spectral imaging (SI) for fluorescence imaging of quantum dots (QDs) in three distinct imaging instruments: eXplore Optix (TDI, Advanced Research Technologies Inc.), Maestro (SI, CRi Inc.), and IVIS-Spectrum (SI, Caliper Life Sciences Inc.).

Procedure: The instruments were compared for their sensitivity in phantoms and living mice, multiplexing capabilities (ability to resolve the signal of one QD type in the presence of another), and the dependence of contrast and spatial resolution as a function of depth.

Results: In phantoms, eXplore Optix had an order of magnitude better sensitivity compared to the SI systems, detecting QD concentrations of ~40 pM *in vitro*. Maestro was the best instrument for multiplexing QDs. Reduction of contrast and resolution as a function of depth was smallest with eXplore Optix for depth of 2–6 mm, while other depths gave comparable results in all systems. Sensitivity experiments in living mice showed that the eXplore Optix and Maestro systems outperformed the IVIS-Spectrum.

Conclusion: TDI was found to be an order of magnitude more sensitive than SI at the expense of speed and very limited multiplexing capabilities. For deep tissue QD imaging, TDI is most applicable for depths between 2 and 6 mm, as its contrast and resolution degrade the least at these depths.

Key words: Time-domain imaging, Frequency-domain imaging, Quantum dots imaging, Optical tomography, Small animal imaging, Molecular imaging

Introduction

Optical fluorescence imaging has been used extensively for imaging small animals using fluorophores that are biologically targeted to a diseased site (molecular imaging agents) [1]. Traditionally, a molecular imaging agent consists of a signaling component and a molecular targeting component. In a fluorescent imaging agent, the signaling molecule is a fluorophore and the molecular targeting molecule is most commonly an antibody or a small peptide targeted to a protein associated with a disease (e.g., RGD peptide targeted to the integrin $\alpha_v\beta_3$).

There are several approaches for whole animal fluorescence imaging including: continuous wave imaging (CWI), frequency domain imaging (FDI), spectral imaging (SI), and time domain imaging (TDI). In CWI, the subject is illuminated with a broad beam of light tuned to the excitation wavelength of the fluorophore. The emission light

Correspondence to: Sanjiv Sam Gambhir; *e-mail:* sgambhir@stanford.edu

that comes back from the subject passes through an emission filter tuned to the fluorophore emission wavelength and detected by a highly sensitive and low noise charged-coupled device (CCD). In FDI, a source emits light at intensities following a radio frequency sinusoid and illuminates the subject. Measurement of amplitude attenuation and phase delay of emitted fluorescence light as it propagates through tissue, allows tomography of fluorescent sources [2]. A fluorophore excited with intensity-modulated light will emit fluorescence at the same modulation frequency, with amplitude attenuation and phase shift resulting from its typical fluorescence lifetime. Light emerging from the surface is measured by a fast detector and a radio-frequency oscillator to drive the diode laser, providing a reference signal for phase detection [3]. In SI, an image is acquired the same way as in CWI, except that a series of images are taken, each with a different emission filter, making it possible to resolve the signal from multiple fluorophores at the same region of interest. The technique requires predetermining the fluorophores' emission spectra. SI systems are capable of reducing endogenous tissue fluorescence (autofluorescence) effects using spectral information, improving signal to background ratio and, hence, achieving better sensitivity. Lastly, in TDI, a spot on the subject is illuminated with a sub-nanosecond duration laser pulse and a fast detector measures the arrival distribution of photons as a function of time at different locations [4, 5]. A light pulse propagating through the tissue is broadened and attenuated due to scattering and absorption [6]. A fluorophore embedded in the tissue will be excited by this pulse of light and emit a fluorescence pulse with a lifetime decay unique to the fluorophore. In addition to spatial intensity distribution, TDI systems can provide temporal information from which fluorescence lifetime can be derived [5, 7]. Therefore, TDI systems allow simultaneous imaging of fluorophores with different lifetimes even if they have overlapping spectra.

Over the last few years, quantum dots (QDs) have been suggested for fluorescence *in vivo* imaging [8–10]. Using QDs for fluorescence imaging holds great promise for high sensitivity and high specificity molecular imaging. QDs have been used to map sentinel lymph nodes [11], an important process in cancer surgery. This mapping method proved QDs have superior sensitivity and specificity compared to other mapping techniques. The emission wavelength of a QD can be easily controlled so as to allow multiplexing several QDs together. Furthermore, they can be easily conjugated to a targeting molecule [12]. QDs of interest for *in vivo* imaging emit red to infrared light in the range of 600–900 nm where tissue absorption and scattering are minimal [13]. Such wavelengths are considered safe for skin exposure as they are non-ionizing. However, the toxicity of the QD molecule is still under investigation. It was recently reported that some smaller QDs are cleared via the renal system [14].

We have previously compared a TDI system to a CWI system through phantom studies [15] and showed the performance tradeoffs between the instruments for imaging a Cy5.5 fluorophore. In this study, we focus specifically on quantum dots that emit in the near infrared range and investigate the performance of a TDI system and two other leading SI systems. In contrast to the previous study, in this study, multiple QDs in the same object were imaged in order to investigate the multiplexing capabilities of the different instruments. Lastly, this study investigates, for the first time to our knowledge, the sensitivity of the instruments in living mice, which is an essential step as phantom studies do not take many critical factors into account such as tissue autofluorescence.

Methods and Materials

Instrumentation

For the TDI system, we used the commercially available eXplore Optix MX (Advanced Research Technologies-GE Healthcare, St. Laurent, Quebec, Canada). This TDI system was compared to two SI systems: IVIS-Spectrum (Xenogen Corporation–Caliper, Alameda, CA, USA) and Maestro (CRi, Woburn, MA, USA).

TDI System The eXplore Optix system uses a fixed pulsed laser diode as an illumination source with excitation wavelengths of either: 635 nm, 670 nm, 735 nm, and 785 nm. The pulse width is less than 150 psec. The system originally supported laser repetition rate of 80 MHz which allows imaging of fluorophores with lifetime of up to ~10 ns. Imaging QDs requires a lower repetition rate as their lifetimes can reach up to 100 ns. Therefore, the repetition rate of the system was adjusted to 2.5 MHz to support fluorescence lifetimes of up to 400 ns. The average laser power can be tuned up to 500 μW or 25.8 μW at repetition rates of 80 MHz or 2.5 MHz, respectively. A galvomirror is used to perform a raster scan of the selected region of interest (ROI) with a step size ranging from 0.5 to 3 mm and a spot size of 1 mm at the image plane. A second galvomirror collects the emanating light, 3 mm away from the illumination point, through an emission filter blocking light at the excitation wavelength with optical density equals to 9. A photomultiplier tube (PMT) coupled to a time-correlated single photon counting system collects the light allowing dynamic detection of the fluorescence signal with a temporal resolution of 250 ps. The dynamic range of the PMT is 16,000, from a dark current level of 125 ph/s (photons per second) to a saturation value of 2,000,000 ph/s and a dead time of 125 ns. In addition, a second camera is incorporated into the system to perform a profilometric scan to render the three-dimensional (3D) surface topography of the subject under study. Data analysis and fluorescence lifetime parameters are obtained using the system's software (eXploreOptix analysis workstation 2.00.00). A fluorescence lifetime map is obtained by fitting the tail of the photon temporal distribution curve and obtaining the characteristic decay time at each point. The eXplore Optix software package includes a 3D concentration reconstruction algorithm that uses an iterative inverse solution to the Born approximation of the diffusion equation for photon density waves in a homogenous scattering medium [16].

In this study, the image acquisition in the eXplore Optix system included a profilometric scan, two-dimensional scan ROI with

1-mm step size and point integration time 0.1–1 s. Repetition rate of 2.5 MHz was chosen so to allow 400 ns for the QDs fluorescence to decay before the next excitation pulse. The laser power is automatically chosen by the acquisition software as the highest power that does not saturate the photon detector. We used an excitation laser at a wavelength of 635 nm for exciting either 705 nm or 800 nm QDs. We used a band-pass emission filter (731± 15 nm) to image 705 nm QDs in the presence of 800 nm QDs and a long-pass filter (693 nm) when 800 nm QDs were not present in the background. A long-pass emission filter (770 nm) was used to image 800 nm QDs.

SI Systems The IVIS-Spectrum system uses a continuous wave quartz halogen lamp generating a constant 150 W broadband light that simultaneously and uniformly illuminates the whole field of view. The light is spectrally filtered for fluorescence excitation with an integrated 12-position excitation wheel containing filters covering a wide spectral range between 415 and 760 nm, each with 30 nm bandwidth. Fluorescent light is collected through a 24-position emission filter wheel covering the spectral range between 490 and 850 nm, each with 20-nm bandwidth. The filters have an optical density of 9 at the excitation wavelength, and imaged by an f/1–f/8, 50 mm lens, at 20 μm pixel size, 2,048 × 2,048 pixels imaging and cryogenically cooled (to −90 C), and 16-bit CCD camera with minimum detectable luminance of 70 photons/s/sr/cm^2. Five interchangeable lenses adjust the field of view, 4–26 cm, between high resolution and high throughput applications. Image analysis is performed by the system software (Living Image 3.0). The main advantage of the IVIS-Spectrum over its predecessor, the IVIS-200, is the spectral imaging capability that allows multiplexing several fluorophores together as well as to reduce autofluorescence signal from the image. The analysis software allows un-mixing of the acquired fluorescent signal given the fluorophores' emission spectra. In this study, we used an excitation filter centered at 640 nm with 30-nm bandwidth, and a set of emission filters all with bandwidth of 20 nm covering the range of 670 to 850 nm. The lamp level was set to high, binning to medium (2 pixels binning), field of view to 6.4–12.3 cm depending on object size, *f* number to 2, and exposure time to 0.5–10 s such that no saturation occurred in the image.

The Maestro system consists of a 300 W xenon-based excitation light source with seven possible excitation and emission filter pairs, covering the complete spectral range from 500 to 950 nm. The fluorescent light emitted from the sample is detected through a long-pass emission filter (matched to the excitation filter) and a macro-lens and the liquid crystal tunable filter (LCTF) which provides a blocking of 9 OD (optical density) at the excitation wavelength, and a 1,392 × 1,040 pixel, cooled, 1.4 megapixel, and 12-bit scientific-grade CCD camera. The LCTF allows the system to spectrally sample more wavelengths compared to IVIS-Spectrum in an attempt to provide more accurate multiplexing capabilities and background reduction. The Maestro system collects a series of wavelength-specific images across the spectral range of interest, and then puts them together into a dataset called a "spectral cube" that contains point-by-point spectral information in an image format through the use of LCTF technology [17]. Every pixel's spectrum can be analyzed by a process called spectral unmixing, in which the signals from the various fluorophores are separated. By utilizing the spectral signatures of the tissue autofluorescence and the fluorophore(s) of interest, the Maestro software quantifies each pixel and determines relative concentrations of the fluorophores present in that pixel [18, 19]. In this study, QDs were excited with a 640-nm excitation filter with 50-nm bandwidth, and a 700-nm long-pass emission filter. The LCTF was scanned across the range of 680 to 950 nm. Exposure time was set as the highest exposure time that did not cause saturation in the ROI and field of view was set to 6.4–12.3 cm depending on the object size.

Phantom Materials

The liquid phantom is composed of 1% Liposyn II (Abbott Laboratories) with a scattering coefficient, μ'_s=1 mm^{-1} [20], similar to that of tissue and with negligible absorption. We used QDs from Invitrogen Corporation (Carlsbad, CA, USA) model: QDot^{TM} 705 nm and 800 nm. The sensitivity and multiplexing experiments were done in a standard 96-well plate.

Animals

All animal experiments were performed in compliance with the Guidelines for the Care and Use of Research Animals established by the Stanford University Animal Studies Committee. For this study, we used 6–8-weeks-old female nude mice from Charles River Laboratories Inc. (Wilmington, MA, USA).

Results

We compared the following instruments: eXplore Optix (TDI), Maestro (SI), and IVIS-Spectrum (SI). The instruments were evaluated for their sensitivity, multiplexing capabilities, depth of detection, and resolution as a function of the depth of the object using liquid phantoms. Furthermore, sensitivity was evaluated in living mice to account for autofluorescence of tissue.

Sensitivity and Linearity

Sensitivity is one of the most important specifications of a fluorescence-imaging instrument. In this paper, sensitivity is defined as the concentration where the linear fitting of the signal to background curve equals 1. The sensitivity is primarily instrument-dependent but also may depend on the fluorophore spectral properties, fluorophore brightness, and tissue background (e.g., autofluorescence). We prepared a serial dilution of 705 nm and 800 nm QDs in water at concentrations varying between 100 fM and 1 μM increasing in multiples of 3. Fifty-microliter triplicates of the same concentration were filled in a 96-well plate and imaged using the three instruments. Figures 1a,b show the signal to background ratio for each instrument as a function of the QDs concentration. Background is defined as the fluorescence signal detected from a well filled with water only. We define the lowest detectable fluorophore concentration as the highest concentration at which the signal to background ratio equals to 1. The linearity of an instrument was measured by the

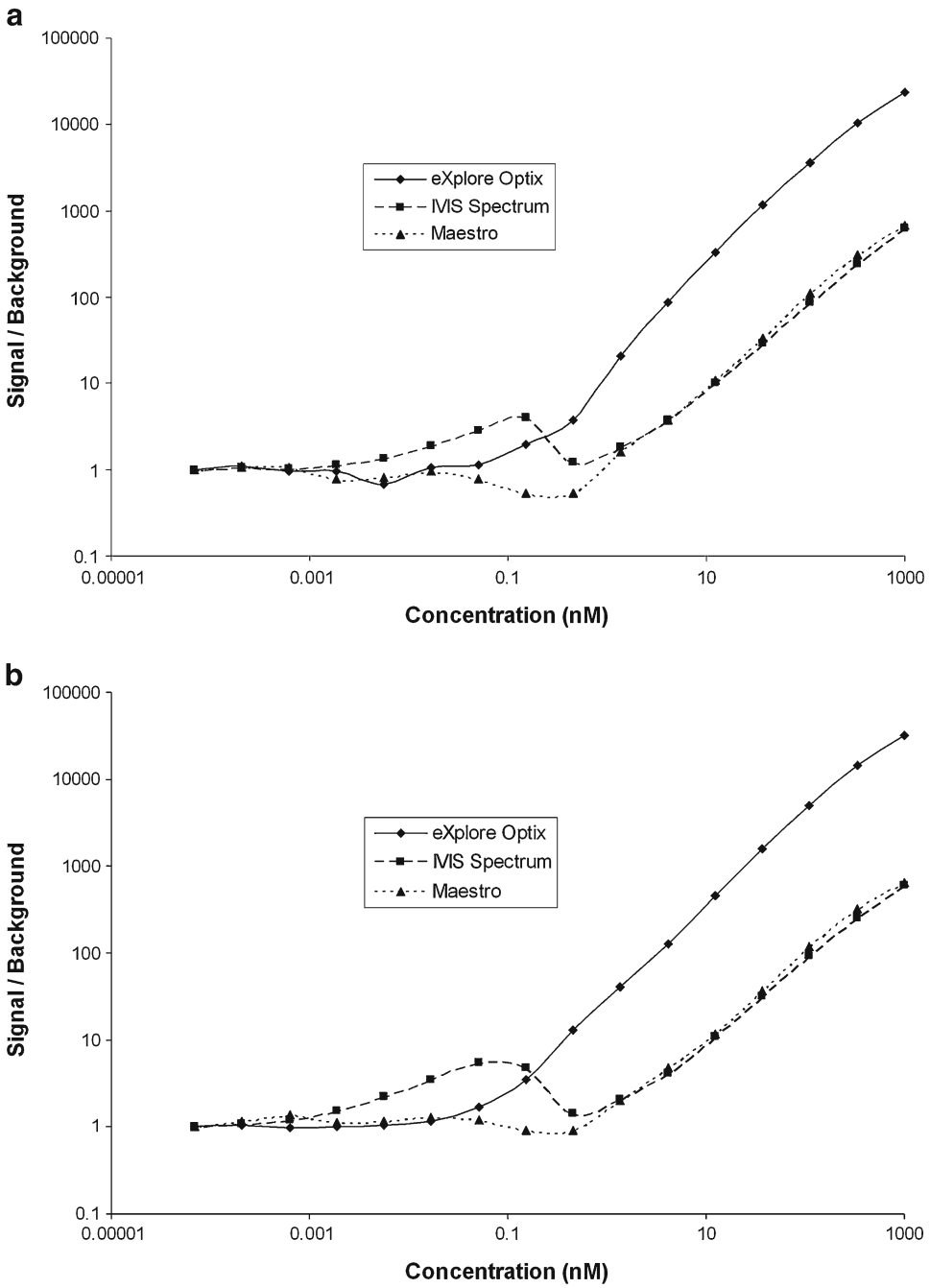

Fig. 1. Signal to background as a function of the concentration of **a** 705 nm QDs and **b** 800 nm QDs. The sensitivity is defined as the concentration where the linear fitting of the signal to background curve equals to 1. The IVIS-Spectrum data shows nonlinearity at 0.1 nM due to an inherently inhomogeneous background signal potentially caused by angle dependency of the emission filter. The standard errors were negligibly small and therefore are not shown here.

coefficient of determination (R^2) of the signal to background graph in the area above the sensitivity limit.

Table 1 summarizes the sensitivity and linearity as measured for the two types of QDs across the three instruments. The eXplore Optix shows an order of magnitude better sensitivity compared with IVIS-Spectrum and Maestro: 70 pM *versus* 460 pM and 640 pM, respectively, for the 705 nm QDs and 37 pM *versus* 640 pM and 620 pM for the 800 nm QDs. The emission filter closest to the peak emission wavelength for the fluorophore of interest was used. Inhomogeneous background signal was observed in the IVIS-Spectrum system from wells that were positioned towards the edges of the field of view of the instrument. This resulted in a nonlinear hill that is observed at concentrations of ~0.1 nM. We believe this could be a result of angle dependency of the emission filter to incident light. Linearity was observed in all instruments at concentrations above the estimated sensitivity limit.

Table 1. Summary of results from the sensitivity and linearity study showing the lowest detectable concentration of quantum dots (QDs). Linearity is quantified as R^2 for concentrations above the sensitivity limit

Instrument	Phantom sensitivity		Linearity (R^2)	
	705 nm	800 nm	705 nm	800 nm
eXplore Optix	70 pM	40 pM	0.993	0.998
IVIS-Spectrum	460 pM	640 pM	0.991	0.995
Maestro	640 pM	620 pM	0.999	0.996

Multiplexing Capabilities

Simultaneous imaging of several QDs in the same subject using the same excitation light is one of the main advantages of QDs over other fluorophores used in molecular imaging. Here, we study the instruments' multiplexing capabilities by quantifying their ability to detect small concentrations of one type of QD in the presence of a higher concentration of another type of QD.

We prepared a serial dilution of 705 nm and 800 nm QDs in water and mixed them in different ratios. First, 800 nm QD concentration was varied between 76 pM and 0.5 μM increasing in multiples of 3 while keeping the 705 nm QDs concentration at 0.5 μM. As a control solution, 705 nm QDs were mixed with water to a concentration of 0.5 uM. Triplicates of the mixtures were put in a 96-well plate (50 uL per well). The multiplexing limit for 800 nm QDs was defined as the ratio between the concentration of 800 nm QDs and 705 nm QDs where the signal from the well containing a mixture was equal to the signal from the control well. The multiplexing limit for 705 nm QDs was obtained similarly.

The multiplexing limits are summarized in Fig. 2. The Maestro system significantly outperformed the eXplore Optix and IVIS-Spectrum, possibly due to its liquid crystal tunable filter increasing spectral sampling of the image. eXplore Optix's multiplexing method suffered from the similarity in lifetimes of the two QDs which resulted in poorer multiplexing capabilities.

Depth of Detection

Evaluation of the largest depth for detecting a signal provides a good estimate of the imaging capabilities in deep tissues. Furthermore, inability to localize signals from deep tissues damages the instrument's sensitivity. A liquid phantom was constructed of a cylindrical container filled with 1% Liposyn (Abott Laboratories), simulating the tissue scattering coefficient 1 mm^{-1}. A cylindrical inclusion with 3-mm diameter was filled with 10 μl of 800 nm QDs at 50 nM and placed at the bottom of the container (Fig. 3a). The liquid level was increased from 0 to 12 mm with steps of 1 mm and accuracy of ±0.1 mm to obtain different inclusion depths.

Figure 3c shows the signal to background ratio as a function of the inclusion depth as measured by the instruments. The signal is defined as the total signal over a circular area, 3 mm in diameter, centered above the inclusion, and the background is defined as the total signal arriving from the entire container. This effectively estimates the ability to localize signals originating from the tissues. The contrast of the eXplore Optix was superior to the Maestro and the IVIS-Spectrum systems. For example, at 2-mm depth the eXplore Optix system showed 65% of the signal as coming from the cylindrical inclusion *versus* only 43% and 30% in the IVIS-Spectrum and Maestro systems, respectively. Despite outperforming the other instruments at the lower depths, the eXplore Optix signal is rapidly dispersing over depth. At 6-mm depth, the image it provides is comparable to the IVIS-Spectrum image. Nonetheless, the Maestro system had the poorest signal to background ratio throughout the depths, and, therefore, the poorest ability to resolve small signals from deep tissues.

Spatial Resolution

Strong light scattering by tissues is the limiting factor for spatial resolution in fluorescence imaging, resulting in poor size quantification of a target [21]. Here, we measure the spatial resolution by placing two capillary tubes, with 0.5-mm inner diameter and 0.2 mm wall thickness, filled with 2 μl volume of 50 nM 800 nm QDs in a liquid-simulating tissue-scattering properties and no absorption. The tubes are positioned in a V-shape such that the distance between the QDs varied between 0.5 and 20 mm (Fig. 4a). By adding liquid to the container, various depths were achieved without moving the tubes themselves. For each depth, we found the point between the tubes at which fluorescence intensity reached 90% of the peak value and defined the resolution to be the distance between the tube at that point. For shorter distances, the two tubes cannot be distinguished from one another.

Figure 4c illustrates the spatial resolution as a function of depth for all three instruments. At zero depth, the IVIS-Spectrum and Maestro have a spatial resolution of less than 0.5 mm, while the eXplore Optix resolution is limited to not less than 1 mm due to its optical spot size of 1 mm. However, beyond a depth of 1 mm the eXplore Optix resolution was significantly better than that of the IVIS-Spectrum and the Maestro systems. At depth of 4 mm, the eXplore Optix could resolve features separated 3.5 mm apart, whereas the IVIS-Spectrum and the Maestro systems could only resolve features that were 7 and 7.5 mm apart, respectively. Beyond depths of 7 mm, the resolution exceeded 10 mm in all instruments.

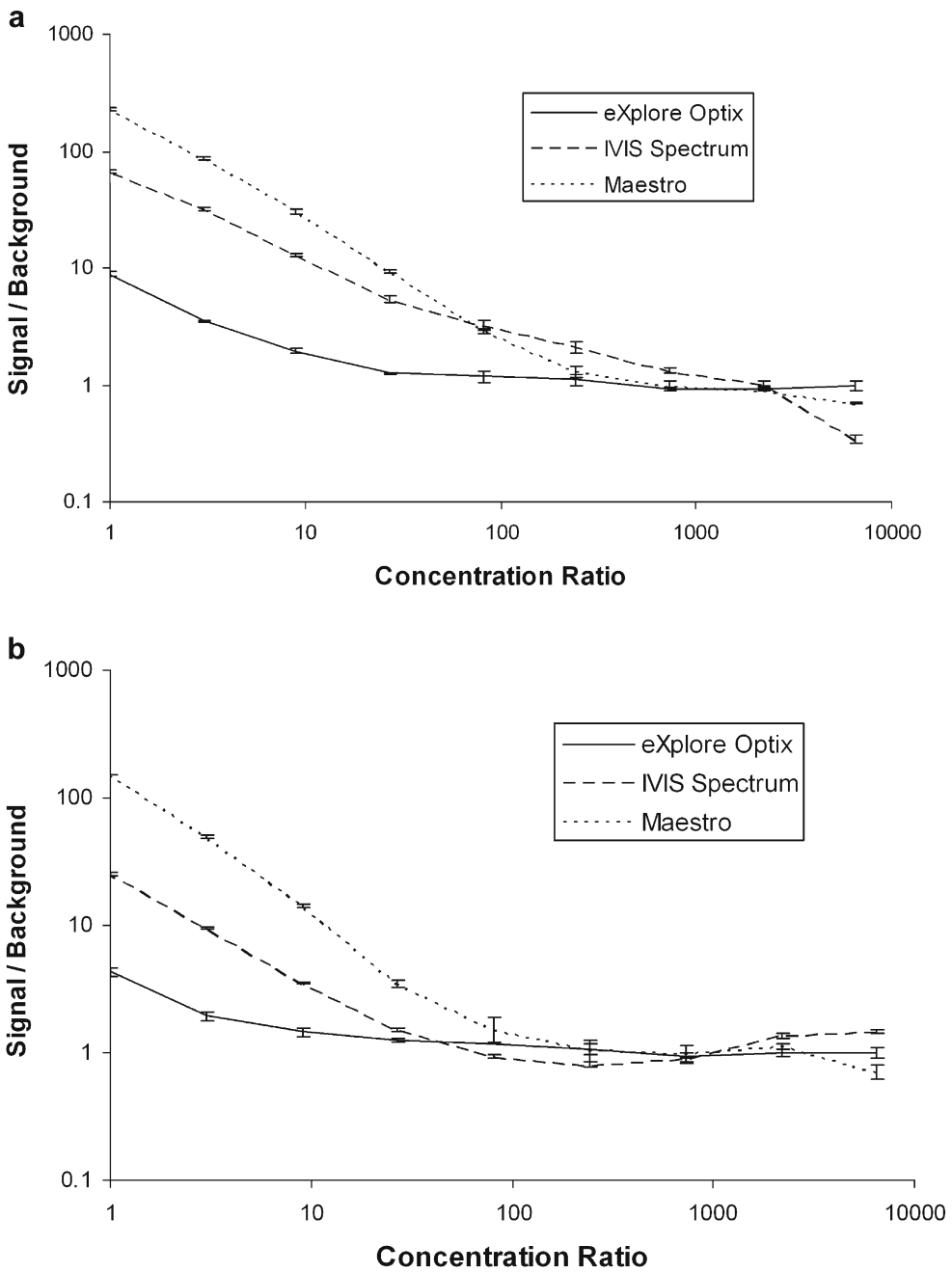

Fig. 2. Multiplexing capabilities defined as the ratio in concentration between the QD of interest for imaging and the background QD. In **a** 705 nm QD concentration is decreasing while the concentration of the background 800 nm QDs stays constant. Likewise, in **b**, 800 nm QDs concentration is diluted while the background 705 nm QDs concentration is maintained constant. The *error bars* represent the standard error ($n=3$).

Sensitivity in Small Animals

A physical phantom is restricted in its ability to measure the true sensitivity limit of a given instrument, primarily because it does not simulate the autofluorescence of tissues. We used a mouse model injected with QDs subcutaneously (under the skin) in its hip area to address the *in vivo* sensitivity limits of the instruments. QDs solutions were prepared by mixing 800 nm QDs with Matrigel (Matrigel Basement Membrane Matrix, Phenol Red-free, Becton Dickinson) in 1:1 ratio at seven concentrations from 19 pM to 300 nM increasing in multiples of 5. The matrigel is needed to retain the QDs within the injected area preventing diffusion to adjacent tissues. Nude mice ($n=3$) were injected on the back with 50 μL of the solutions plus a control inclusion containing matrigel only. Figure 5 shows the signal to background ratio as measured from the inclusions. The background level was measured as the average skin signal from a mouse hip that was not injected with QDs. The control inclusion showed similar signal to this background signal. All three systems showed similar sensitiv-

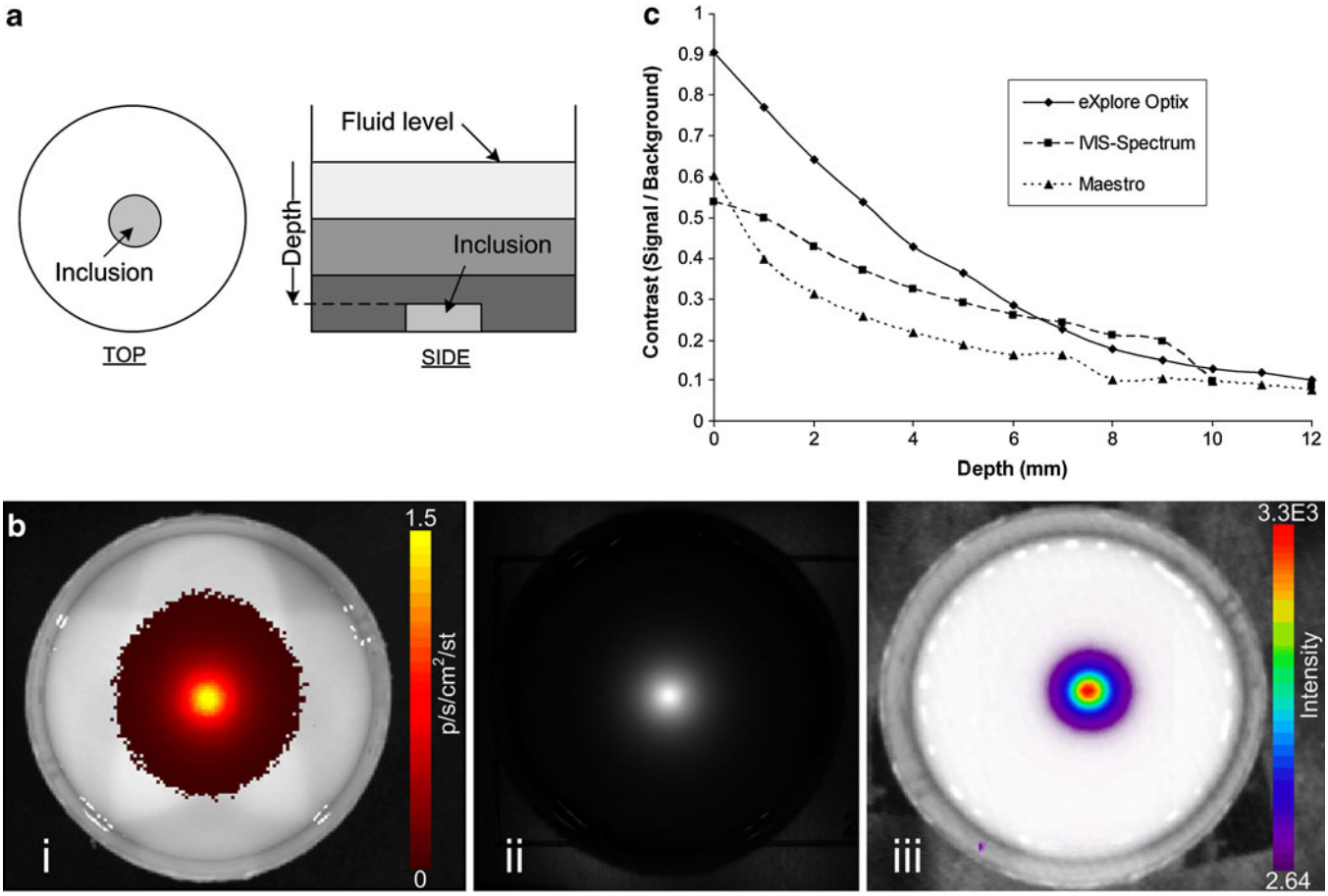

Fig. 3. Contrast as a function of depth. **a** The phantom that was used. **b** The images taken from (*i*) IVIS-Spectrum, (*ii*) Maestro and (*iii*) eXplore Optix at 3-mm inclusion depth. **c** Contrast as a function of depth across the three systems. Contrast is defined as the signal from a region of interest located at the center of the phantom the size of the inclusion (*dotted circle in b*) divided by the overall signal from the phantom.

ities *in vivo*. However, the explore Optix and Maestro systems showed superior contrast compared with IVIS-Spectrum.

Discussion

We have compared three fluorescence imaging systems for imaging of QDs by examining different aspects of their performance. QDs bring promise for highly sensitive and specific molecular imaging applications in living animals. This is due to their easily tunable and narrow emission spectra allowing multiplexing of multiple QDs together using the same excitation wavelength. Furthermore, QDs can be easily conjugated to targeting molecules [5] such as peptides or antibodies. While the results shown in this paper and the conclusions drawn are relevant for the specific imaging systems that were used under the given conditions, more general guidelines for the differences between TDI and SI systems can be drawn.

Sensitivity in phantoms and living mice, multiplexing capability, depth of detection, and spatial resolution were investigated in a series of experiments. The eXplore Optix TDI system was found to be an order of magnitude more sensitive than the IVIS-Spectrum and Maestro SI systems, detecting minute concentrations of 705- and 800-nm quantum dots in a phantom. The signal linearity with respect to QD concentration was similar in all systems. We noticed inhomogeneous background signal in the IVIS-Spectrum system that increases towards the edges of the field of view. It affected the IVIS-Spectrum' sensitivity results such that a hill appeared in the curves representing signal *versus* concentration. We believe this effect is caused by an angle dependency of the emission filter leading to less efficient blocking of the excitation light that is reflected back from the edges of the field of view. Depth of detection and spatial resolution were other criteria showing superiority of TDI compared with SI. This is likely due to the highly distinct illumination methods used in the two types of systems. The eXplore Optix TDI imaging system illuminates a focused point, therefore, having significantly higher power density than wide-area illumination used in the IVIS-Spectrum and Maestro SI systems. The study demonstrates that the spectral imaging systems have superior multiplexing capabilities over the time domain system for imaging multiple QDs.

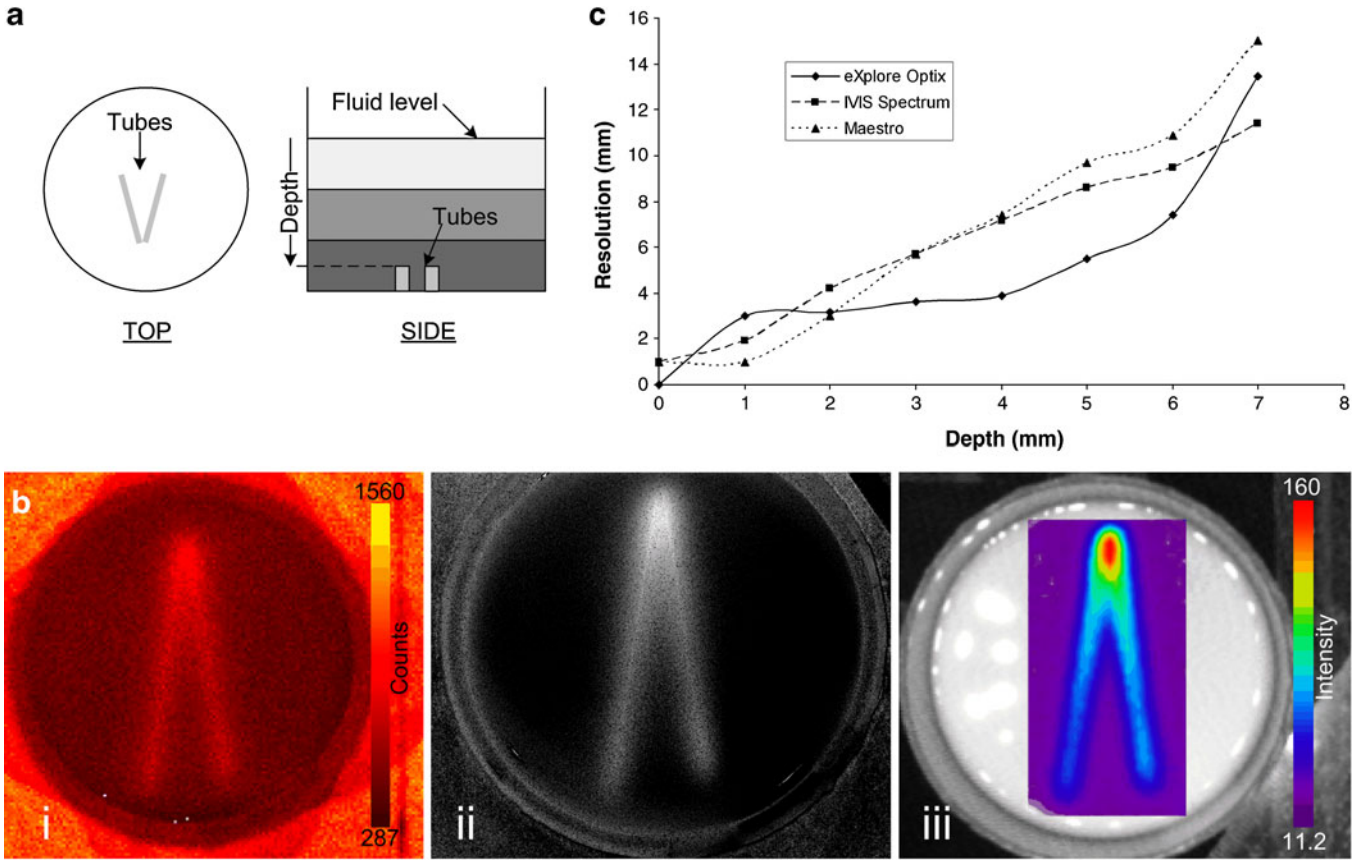

Fig. 4. Resolution as a function of depth. **a** Capillary tubes containing 50 nM of 800-nm QDs were positioned in a V-shape. Resolution was measured as the minimum distance between two points that is separated by a signal 90% as strong as the peak value. **b** Shows images taken from (*i*) IVIS-Spectrum, (*ii*) Maestro, and (*iii*) eXplore Optix at 3 mm inclusion depth. **c** Resolution as a function of depth across the three systems.

This is due to the fact that while different QDs have distinct spectra, their fluorescence emission lifetimes are nearly identical making the lifetime analysis of the eXplore Optix ineffective. Different contrast agents with more distinct fluorescence lifetimes may allow the time domain eXplore Optix system to produce better multiplexing results. Additionally, Maestro demonstrated better multiplexing capabilities compared to IVIS-Spectrum. This can be explained by

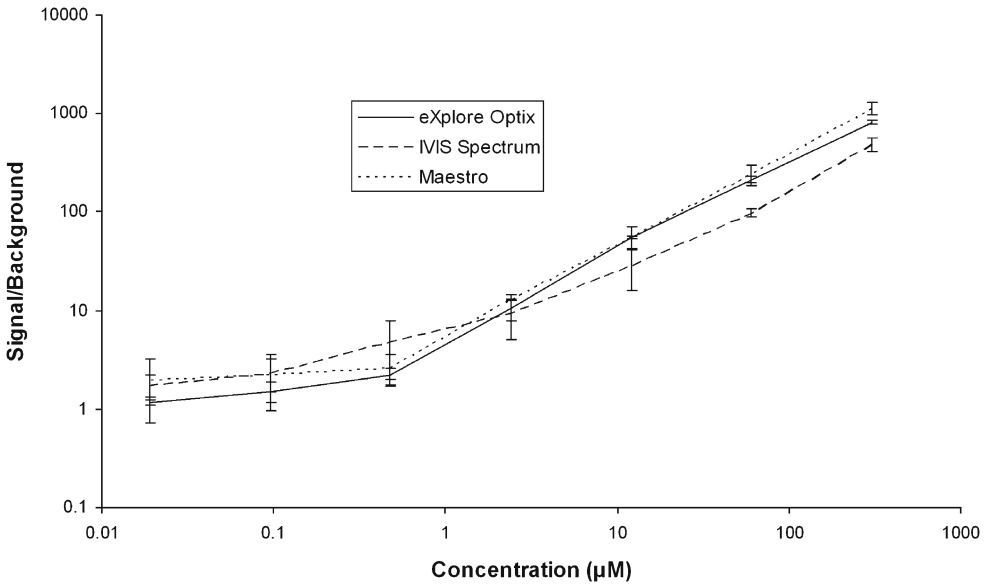

Fig. 5. Signal to background ratio as a function of the concentration of 800 nm QDs injected subcutaneously to living mice. The *error bars* represent the standard error ($n=3$).

Maestro's liquid crystal tunable filter allowing high spectral resolution sampling which evidently leads to better approximation of relative fluorophore concentration. While a notable advantage of the eXplore Optix system is its ability to reconstruct 3D images, it uses a raster scanning method to image the object leading to relatively long acquisition times. For instance, the acquisition time for three rows of 12 wells ranges from 5–50 min depending on the integration time (0.1–1 s) compared to 1 min using the IVIS-Spectrum or 30 s using the Maestro system. Newer software in the eXplore Optix system which were added after the completion of this study, allows faster acquisitions at the expense of degraded image quality (by using lower integration times). The time of acquisition is of particular importance for biodistribution studies where the distribution of an imaging agent in a mouse is monitored over a period of time. To acquire an image of an entire mouse, the eXplore Optix requires approximately 20 min compared to less than a minute with the SI systems. To further evaluate the systems' performance, we tested their sensitivity in living mice, to account for autofluorescence. The eXplore Optix and Maestro systems displayed similar sensitivity *in vivo* between themselves and superior contrast compared to the IVIS-Spectrum system. The performance difference between the SI systems is explained by the superior multiplexing capabilities of the Maestro system allowing to filter out the tissue autofluorescence better. The sensitivity and contrast measurements of QDs agree well with the sensitivity and contrast measurements in an earlier report by our lab [15] using small molecule-based fluorescent dyes in phantoms. However, the small molecule-fluorescent dye study did not address multiplexing capabilities and sensitivity in living animals. This study shows significantly different results in animals than tissue mimicking phantoms, likely due to autofluorescence.

Conclusion

In our experiments, the benefits and drawbacks of two common fluorescent imaging modalities, time domain imaging, and spectral imaging were made apparent. *In vitro*, TDI was found to be more sensitive than SI at the expense of lower speed of acquisition and very limited multiplexing capabilities. *In vivo*, both modalities had comparable sensitivity capabilities. SI demonstrated significantly better multiplexing capabilities of quantum dots over TDI. Within the SI systems, higher spectral resolution significantly enhanced multiplexing performance leading to better multiplexing capabilities of the Maestro system compared with the IVIS-Spectrum system. For deep tissue QD imaging, TDI showed significantly better contrast and spatial resolution than the SI systems for depths between 2 and 6 mm.

Acknowledgements. We acknowledge funding support from the National Institute of Health grants NCI CCNE U54 CA119367 (SSG), NCI ICMIC P50 CA114747 (SSG) and the Canary Foundation (SSG). A. de la Zerda thanks the Bio-X Graduate Student Fellowship and the DoD Breast Cancer Research Program - Predoctoral Traineeship Award for partially supporting this work.

References

1. Massoud TF, Gambhir SS (2003) Molecular imaging in living subjects: seeing fundamental biological processes in a new light. Genes Dev 17:545–580
2. Lee J, Sevick-Muraca EM (2002) Three-dimensional fluorescence enhanced optical tomography using referenced frequency-domain photon migration measurements at emission and excitation wavelengths. J Opt Soc Am A, Opt Image Sci Vis 19:759–771
3. Godavarty A, Eppstein MJ, Zhang C, Theru S, Thompson AB, Gurfinkel M, Sevick-Muraca EM (2003) Fluorescence-enhanced optical imaging in large tissue volumes using a gain-modulated ICCD camera. Phys Med Biol 48:1701–1720
4. McCormack E, Micklem DR, Pindard LE, Silden E, Gallant P, Belenkov A, Lorens JB, Gjertsen BT (2007) *In vivo* optical imaging of acute myeloid leukemia by green fluorescent protein: time-domain autofluorescence decoupling, fluorophore quantification, and localization. Mol Imaging 6:193–204
5. Kumar AT, Skoch J, Bacskai BJ, Boas DA, Dunn AK (2005) Fluorescence-lifetime-based tomography for turbid media. Opt Lett 30:3347–3349
6. Arridge SR, Hebden JC (1997) Optical imaging in medicine: II. Modelling and reconstruction. Phys Med Biol 42:841–853
7. Elson D, Requejo-Isidro J, Munro I, Reavell F, Siegel J, Suhling K, Tadrous P, Benninger R, Lanigan P, McGinty J, Talbot C, Treanor B, Webb S, Sandison A, Wallace A, Davis D, Lever J, Neil M, Phillips D, Stamp G, French P (2004) Time-domain fluorescence lifetime imaging applied to biological tissue. Photochem Photobiol Sci 3:795–801
8. Cai W, Shin DW, Chen K, Gheysens K, Cao Q, Wang SX, Gambhir SS, Chen X (2006) Peptide-labeled near-infrared quantum dots for imaging tumor vasculature in living subjects. Nano Lett 6:669–676
9. Li ZB, Cai W, Chen W (2007) Semiconductor quantum dots for *in vivo* imaging. J Nanosci Nanotechnol 7:2567–2581
10. Gao X, Chung LW, Nie S (2007) Quantum dots for *in vivo* molecular and cellular imaging. Methods Mol Biol 374:135–145
11. Kim S, Lim Y,Soltesz E, De Grand A, Lee J, Nakayama A, Parker J, Mihaljevic T, Laurence R, Dor D, Cohn L, Bawendi M, Frangioni J (2004) Near-infrared fluorescent type II quantum dots for sentinel lymph node mapping. Nat Biotechnol 22:93–97
12. Cai W, Chen X (2008) Preparation of peptide-conjugated quantum dots for tumor vasculature-targeted imaging. Nat Protoc 3:89–96
13. Weissleder R, Ntziachristos V (2003) Shedding light onto live molecular targets. Nat Med 9:123–128
14. Soo Choi H, Liu W, Misra P, Tanaka E, Zimmer JP, Itty Ipe B, Bawendi MG, Frangioni JV (2007) Renal clearance of quantum dots. Nat Biotechnol 25:1165–1170
15. Keren S, Gheysens O, Levin CS, Gambhir SS (2008) A comparison between a time domain and continuous wave small animal optical imaging system. Medical Imaging, IEEE Transactions on 27:58–63
16. Lam S, Lesage F, Intes X (2005) Time domain fluorescent diffuse optical tomography: analytical expressions. Opt Express 13:2263–2275
17. Miller PJ, Hoyt CC (1995) Multispectral imaging with a liquid crystal tunable filter. Presented at Optics in Agriculture, Forestry, and Biological Processing, Boston, MA
18. Levenson RM, Lynch DT, Kobayashi H, Backer JM, Backer MV (2008) Multiplexing with multispectral imaging: from mice to microscopy. Ilar J 49:78–88
19. Mansfield JR, Gossage KW, Hoyt CC, Levenson RM (2005) Autofluorescence removal, multiplexing, and automated analysis methods for *in vivo* fluorescence imaging. J Biomed Opt 10:41207
20. Godavarty A, Sevick-Muraca EM, Eppstein MJ (2005) Three-dimensional fluorescence lifetime tomography. Med Phys 32:992–1000
21. Chernomordik V, Gandjbakhche A, Lepore M, Esposito R, Delfino I (2001) Depth dependence of the analytical expression for the width of the point spread function (spatial resolution) in time-resolved transillumination. J Biomed Opt 6:441–445